Supplementary Information: Understanding Energy Level Alignment in Donor-Acceptor/Metal Interfaces from Core-Level Shifts

*Afaf El-Sayed,[1‡] Patrizia Borghetti,[2,3‡] Elizabeth Goiri,[2‡] Celia Rogero,[2,3] Luca Floreano,[4] Giacomo Lovat,[4] Duncan John Mowbray,[2,5] Jose Luis Cabellos,[2,5] Yutaka Wakayama,[6] Angel Rubio,[2, 3, 5] Jose Enrique Ortega,[*1, 2, 3]. Dimas G. de Oteyza[*3,7]*

[1]Dpto. Fisica Aplicada I, Universidad del Pais Vasco UPV/EHU, E-20018 San Sebastian, Spain

[2]Donostia International Physics Center, Paseo Manuel Lardizabal 4, E-20018 San Sebastian, Spain

[3]Centro de Fisica de Materiales CSIC/UPV-EHU-Materials Physics Center, E-20018 San Sebastian, Spain

[4]CNR-IOM, Laboratorio Nazionale TASC, Basovizza SS-14 Km. 163.5, I-34149, Trieste, Italy

[5]Nano-Bio Spectroscopy Group and ETSF Scientific Development Center, Departamento de Fisica de Materiales, Universidad del Pais Vasco UPV/EHU, Avenida de Tolosa 7, E-20018 San Sebastian, Spain

[6]International Center for Materials Nanoarchitectonics (WPI-MANA), National Institute for Materials Science, 1-1 Namiki, Tsukuba 305-0044, Japan

[7]University of California at Berkeley, Department of Physics, Berkeley, CA 94720, USA

* e-mail: enrique.ortega@ehu.es; d_g_oteyza@ehu.es

Contents

1. Crystalline Structure of Molecular Blends.

Molecular blends self-assemble forming networks that lie flat on the metal surface. The complete collection of STM images of the crystalline structures observed as a function of the donor-acceptor ratio on the various substrates is shown in Fig. S1. The structural details of some of these superlattices have been discussed previously. [1-3] Intermolecular hydrogen bonds stabilize a number of different structures. However, only in the 1:1 ratio, which provides the highest donor-acceptor interface and the highest density of hydrogen bonds, we find the same crystalline structure regardless of the molecular combination or substrate. This indicates the dominant role of intermolecular interactions (including steric contributions, van der Waals and hydrogen bonds) in the determination of the resulting structure. The only exception is a minor rearrangement observed for F_{16}CuPc-PEN on the most interacting of our surfaces, namely Cu(111). However, for other molecular ratios with consequently lower density of hydrogen bonds and therefore weaker intermolecular interactions, we find varying (or simply non-crystalline) structures or segregation. The structures that have been used for spectroscopic characterization are highlighted with green frames. The molecule-substrate distances available in the literature for single-component layers as measured by X-ray standing waves are included in the figure taking as a reference the height of the molecular C backbone. [4-9]

The molecules in combinations of CuPc and PEN are isomorphic to those of F_{16}CuPc with PEN or CuPc with PFP. However, the former corresponds to a donor-donor combination and lacks the strong intermolecular interactions resulting from hydrogen bonds. As a consequence, and in contrast to the donor-acceptor combinations, CuPc-PEN molecular blends tend to segregate into single component domains or striped patterns, as shown in Fig. S2 or as previously reported for comparable blends combining CuPc with di-indenoperylene (DIP). [10]

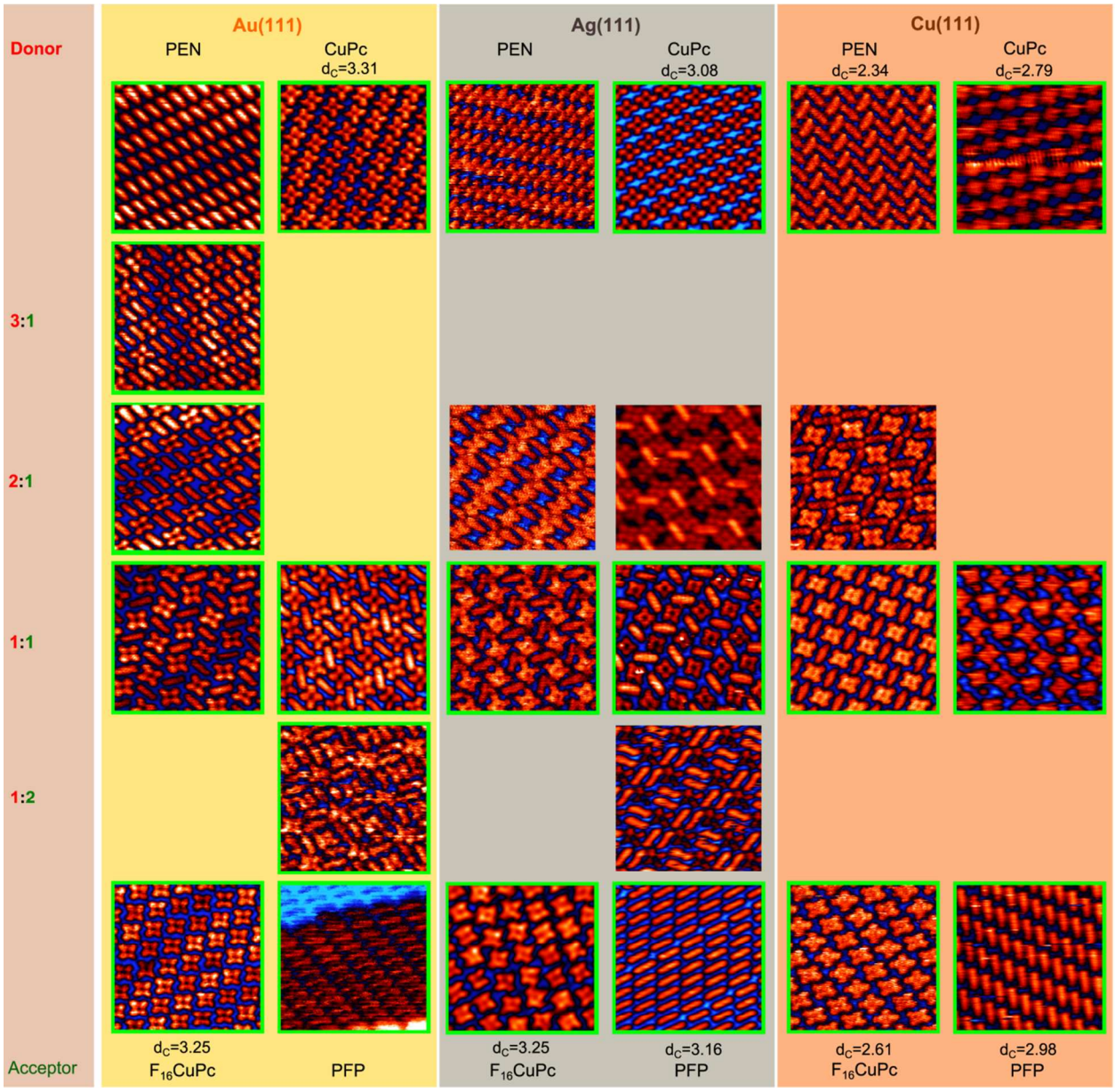

Figure S1. Constant current STM images (9.5 x 9.5 nm^2) of the collection of crystalline structures observed amongst the full variety of interfaces resulting from the two donor-acceptor combinations on the different surfaces and varying stoichiometry (indicated in the left as donor:acceptor). The height of the molecular C backbone as measured by X-ray Standing Waves is included in the figure for those single-component monolayers with available published data.

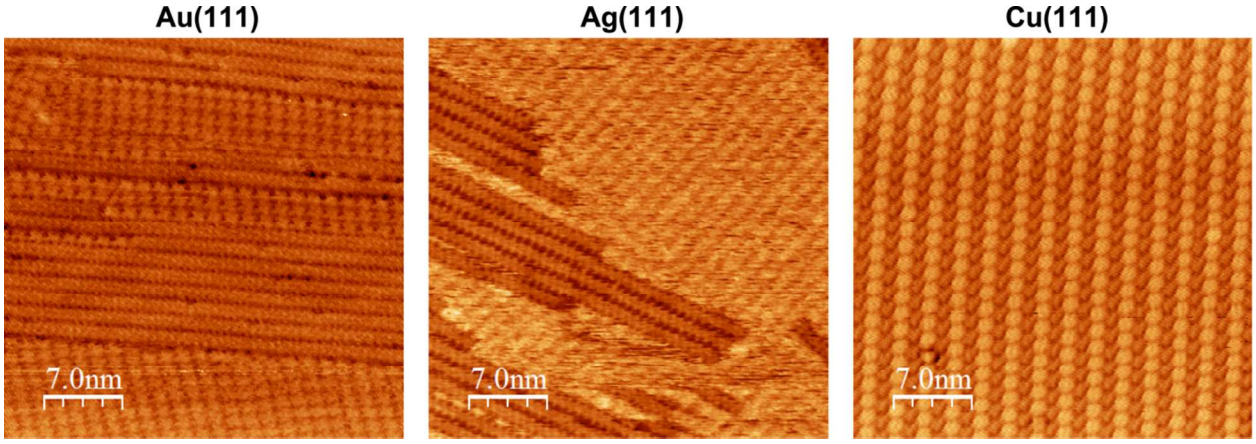

Figure S2. Constant current STM images of CuPc-PEN blends on Au(111), Ag(111) and Cu(111) surfaces, exhibiting phase separation into pure single molecule phases on Au and Ag and striped crystalline blends on Cu (upon gentle annealing to 60 °C).

2. HOMO and LUMO Level Alignment

The HOMO of each molecule has been determined and distinguished from interfacial hybrids by comparison with multilayer spectra. The spectra of monolayer (ML) and multilayer films of single component F_{16}CuPc and PEN films on Au(111) are shown in Fig. S3. Overlaid is the signal of the clean Au(111) substrate, appropriately scaled considering the attenuation by the overlayer. We assume that all ML structures attenuate the valence band emission of Au by the same amount, such that the Au Fermi edge fits to the featureless edge of the F_{16}CuPc ML spectrum. A similar procedure for the PEN ML spectrum can be discarded for various reasons. First, it shows unambiguous features and does not fit the scaled Au spectrum as a result of the interface gap states. Second, the higher electron density in F_{16}CuPc layers (~2 $e^-/Å^2$ vs ~1.25 $e^-/Å^2$ as calculated from their respective unit cells in monolayers) seems contradictory with a higher attenuation from PEN layers. With this criterion, the intensity of F_{16}CuPc fluorine 2p levels around 10 eV (where PEN basically doesn't emit) scales consistently with the varying fluorine coverage in different blends. The spectra of the various films after subtraction of the substrate signal are shown below, together with their respective fits. We remark that this spectral subtraction analysis is limited to the VB range corresponding to the *sp* plateau of the metal substrate and at a kinetic energy >130 eV, thus excluding the emergence of spurious states due to the photoelectron diffraction phenomena.[11] In agreement with previous work by Koch et al. the PEN HOMO is assigned to the peak shadowed red. [12] Instead, the features closer to E_F observed in the ML spectrum disappear for multilayers and are hence assumed to be interface hybrids.[13] In the case of F_{16}CuPc, the HOMO in the multilayer is observed at 1.15 eV. Previous work by Shen and Kahn showed all molecular orbitals and core levels of F_{16}CuPc on Au(111) to shift by 0.3 eV when comparing mono- and multilayers as a result of a decreased screening of the photoinduced hole with increasing distance to the metal substrate. [14] That shift coincides with the difference in binding energy between the multilayer HOMO and the most intense feature in the ML spectrum, which we therefore assign as the ML HOMO. Again, the feature observed in the monolayer at lower binding energy vanishes in the multilayer spectrum and is hence considered an interface hybrid.

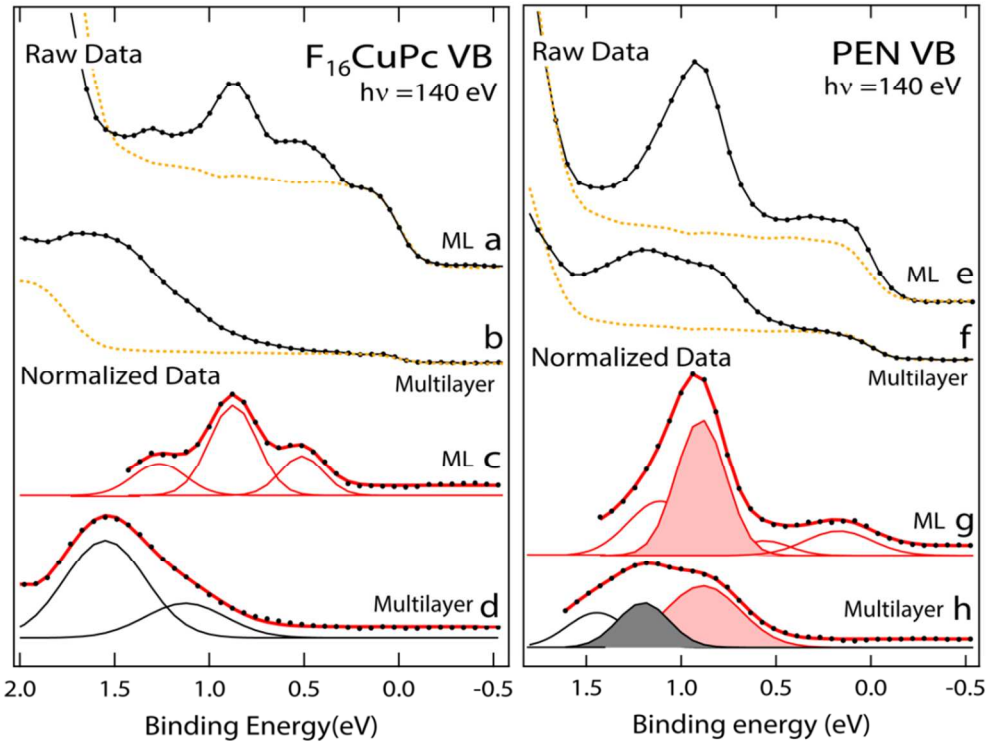

Figure S3. Valence band photoemission spectra of F_{16}CuPc and PEN films on Au(111). (a) and (b) depict the raw data of F_{16}CuPc mono- and multilayer, respectively, while (c) and (d) display the normalized data after subtraction of the appropriately scaled Au(111) signal (yellow dotted lines), together with their fits. (e) and (f) correspond to the raw data of PEN mono- and multilayer, respectively, while (g) and (h) show the normalized data and their fits.

The rigid shift of the unoccupied molecular orbitals together with the core levels is inferred from NEXAFS measurements. NEXAFS measurements were recorded in partial electron yield with an energy resolution of 100 meV. [15] The low-energy secondary electrons were filtered out by means of a negatively polarized grid (-230 V for the carbon edge, -370 V for the nitrogen edge) placed in front of the sample. NEXAFS spectra were taken with the (linear) polarization plane of the light perpendicular to the surface of the sample, while keeping the incidence beam angle at 6°. The raw data were normalized to the total photon flux. The energies in NEXAFS spectra are strongly affected by electron-hole interactions. These hamper an easy access to the real energies of the unoccupied orbitals and the associated charge injection barriers. However, because the exciton binding energy can be considered independent of the molecular surrounding, it is still a reliable technique to probe relative shifts in the orbital energies. We have made use of this capability and summarize the data of F_{16}CuPc-PEN blends on Au(111) as a function of the stoichiometry in Fig. S4. The two molecules hold C atoms, and hence both contribute to the signal in C K-edge NEXAFS spectra. However, comparison of the respective single component layer

spectra evidence that the onset and first subsequent features are solely associated with PEN. Comparing now the spectra of the various blends with that of the pure PEN monolayer we observe an absence of shifts that indicates an unchanged energy difference between the PEN core levels and its unoccupied molecular orbitals. Since we have previously seen the stoichiometry-dependent core-level shifts, we can conclude that the unoccupied orbitals must follow the same shift rigidly.

The same analysis can be easily performed for the F_{16}CuPc orbitals focusing on the N K-edge. Since PEN does not have any N atoms, the signal can be unambiguously assigned to F_{16}CuPc. In addition, it is known from previous works that the F_{16}CuPc LUMO has a strong contribution on the N atoms, making this absorption edge perfectly suited for our aim. [16] Comparison of the various spectra reveals no shifts in the spectra, which in combination with the knowledge of the core-level shifts again leads us to the conclusion that the unoccupied molecular orbitals follow those rigidly.

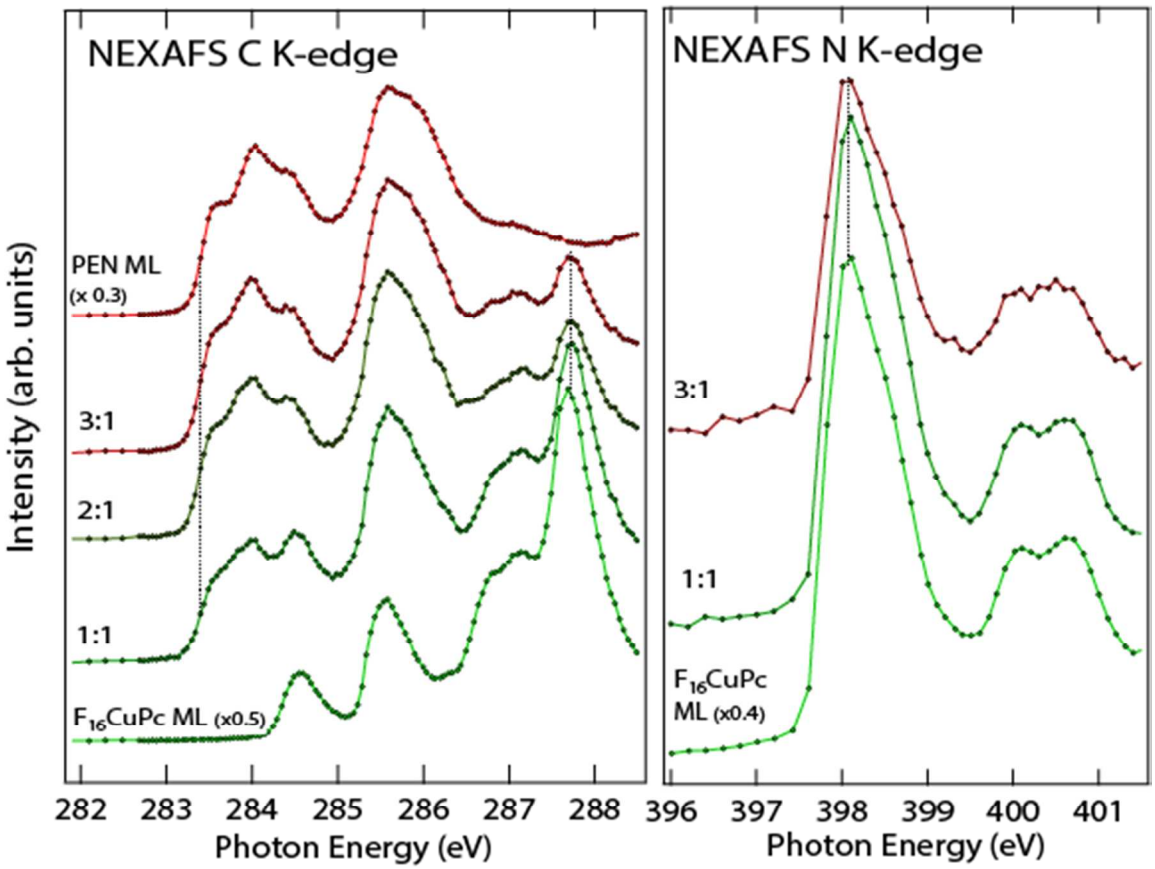

Figure S4. C and N K-edge NEXAFS spectra of F_{16}CuPc-PEN monolayer blends on Au(111) with varying molecular ratio. As a guide to the eye, we include lines connecting the onset of the C K-edge spectra (assigned to PEN), as well as a higher energy resonance in the C K-edge spectrum and the peak position of N K-edge spectra (both assigned to F_{16}CuPc), evidencing the absence of shifts.

3. Intermolecular Charge Transfer

Little effective overlap of σ or π orbitals is typically expected from side-by-side flat-lying molecules. However, the intermolecular electronic coupling is presumably enhanced by the numerous hydrogen bonds present in the blends, which have previously been shown to provide electronic coupling even surpassing that of interfaces composed entirely by C-C σ bonds. [17] Intermolecular hybridization is indeed confirmed from the intermolecular charge transfer obtained from a Bader analysis of the mixed layers, as well as from the spatial distribution of molecular orbitals extending over neighboring molecular species as shown by way of example in Fig. S5.

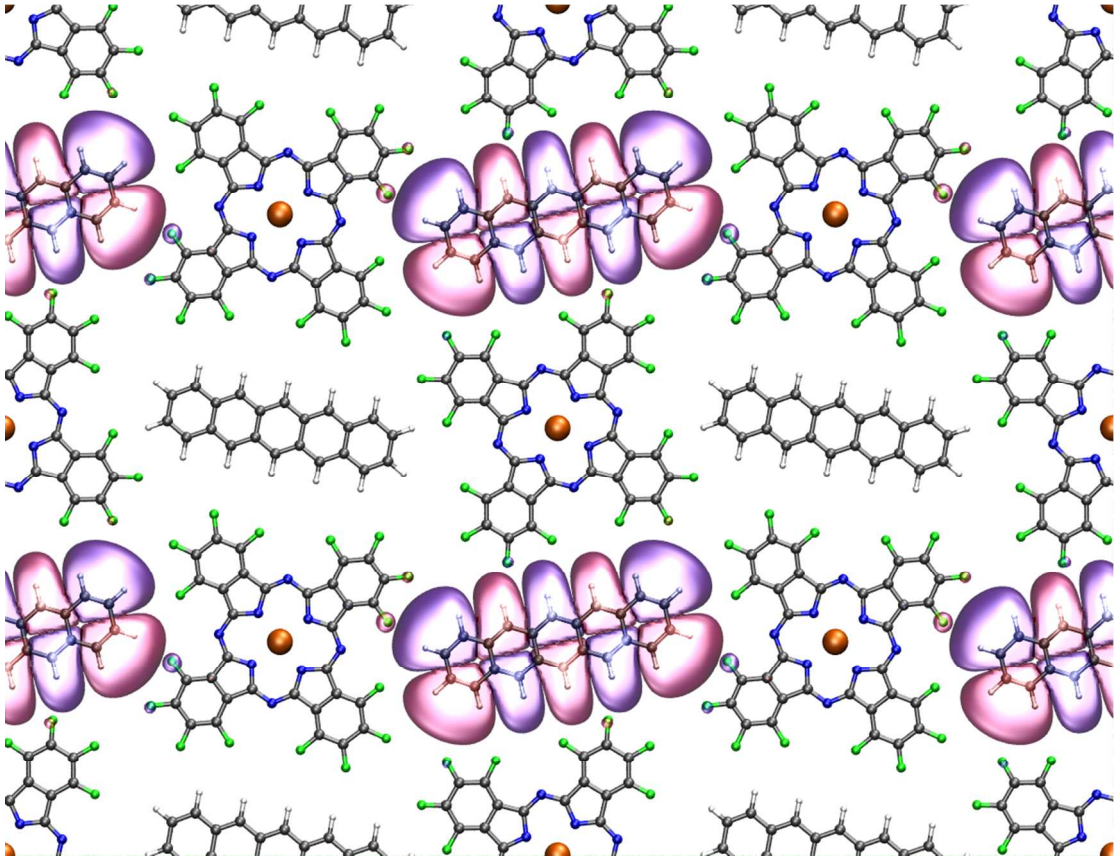

Figure S5. Schematic of the 1:1 PEN:F_{16}CuPc mixture with an isosurface plot at +-0.0005 e/Ang.$^{3/2}$ of the PEN HOMO level. Note the hybridization with the levels of the F atoms of F_{16}CuPC, through which charge transfer occurs. H, C, N, F, and Cu atoms are depicted as white, gray, blue, green, and orange balls, respectively.

[1] Wakayama, Y.; de Oteyza, D. G.; Garcia-Lastra, J. M.; Mowbray, D. J. Solid-State Reactions in Binary Molecular Assemblies of F_{16}CuPc and Pentacene. *ACS Nano* **2011**, *5*, 581-589.

[2] El-Sayed, A.; Mowbray, D.J.; Garcia-Lastra, J.M.; Rogero, C.; Goiri, E.; Borghetti, P.; Turak, A.; Doyle, B.D.; Dell´Angela, M.; Floreano, L.; *et al.* Supramolecular Environment-Dependent Electronic Properties of Metal−Organic Interfaces. *J. Phys. Chem. C* **2012**, *116*, 4780-4785.

[3] Cabellos, J. L.; Mowbray, D.J.,; Goiri, E.; El-Sayed, A.; Floreano, L.; de Oteyza, D.G.; Rogero, C.; Ortega, J.E.; Rubio, A. Understanding Charge Transfer in Donor−Acceptor/Metal Systems: A Combined Theoretical and Experimental Study. *J. Phys. Chem. C* **2012**, *116*, 17991-18001

[4] Koch, N.; Gerlach, A.; Duhm, S.; Glowatzki, H.; Heimel, G.; Vollmer, A.; Sakamoto, Y.; Suzuki, T.; Zegenhagen, J.; Rabe, J.P; *et al*. Adsorption-Induced Intramolecular Dipole: Correlating Molecular Conformation and Interface Electronic Structure. *J. Am. Chem. Soc*. **2008**, *130*, 7300-7304.

[5] Gerlach, A.; Schreiber, F.; Sellner, S.; Dosch, H.; Vartanyants, I.A.; Cowie, B.C.C.; Lee, T.-L.; Zegenhagen, J. Adsorption-Induced Distortion of F_{16}CuPc on Cu(111) and Ag(111): An X-Ray Standing Wave Study. *Phys. Rev. B* **2005**, *71*, 205425-1-7.

[6] Duhm, S.; Hosoumi, S.; Salzmann, I.; Gerlach, A.; Oehzelt, M.; Wedl, B.; Lee, T.-L.; Schreiber, F.; Koch, N.; Ueno, N.; *et al.* Influence of Intramolecular Polar Bonds on Interface Energetics in Perfluoro-Pentacene on Ag(111). *Phys. Rev. B* **2010**, *81*, 045418-1-6.

[7] Kroger, I.; Stadtmuller, B.; Kleimann, C.; Rajput, P.; Kumpf, C. Normal-Incidence X-Ray Standing-Wave Study of Copper Phthalocyanine Submonolayers on Cu(111) and Au(111). *Phys. Rev. B* **2011**, *83***,** 195414-1-9.

[8] Kroger, I.; Stadtmuller, B.; Stadler, C.; Ziroff, J.; Kochler, M.; Stahl, A.; Pollinger, F.; Lee, T.-L.; Zegenhagen, J.; Reinert F.; *et al.* Submonolayer Growth of Copper-Phthalocyanine on Ag(111). *New J. Phys*. **2010**, *12*, 083038-1-23.

[9] de Oteyza, D. G.; El-Sayed, A.; Garcia-Lastra, J.M.; Goiri, E.; Krauss, T.N.; Turak, A.; Barrena, E.; Dosch, H.; Zegenhagen, J.; Rubio, A.; *et al.* Copper-Phthalocyanine Based Metal–Organic Interfaces: The Effect of Fluorination, the Substrate, and its Symmetry. *J. Chem. Phys*. **2010**, *133*, 214703-1-6.

[10] de Oteyza, D. G.; Barrena, E.; Dosch, H.; Ortega, J. E.; Wakayama, Y. Tunable Symmetry and Periodicity in Binary Supramolecular Nanostructures. *Phys. Chem. Chem. Phys*. **2011**, *13*, 4220-4223.

[11] Giovanelli, L.; Bocquet, F.C.; Amsalem, P.; Lee, H.-L.; Abel, M:; Clair, S.; Koudia, M.; Faury, T.; Petaccia, L.; Topwal, D.; *et al*. Interpretation of Valence Band Photoemission Spectra at Organic-Metal Interfaces. *Phys. Rev. B* **2013**, *87*, 035413-1-6

[12] Koch, N.; Vollmer, A.; Duhm, S.; Sakamoto, Y.; Suzuki, T. The Effect of Fluorination on Pentacene/Gold Interface Energetics and Charge Reorganization Energy. *Adv. Mater*. **2007**, *19*, 112-116.

[13] Duhm, S.; Gerlach, A.; Salzmann, I.; Broker, B.; Hohnson, R.L.; Schreiber, F.; Koch, N. PTCDA on Au(111), Ag(111) and Cu(111): Correlation of Interface Charge Transfer to Bonding Distance. *Org. Elect*. **2008**, *9*, 111-118.

[14] Shen, C.; Kahn, A. Electronic Structure, Diffusion, and p-Doping at the Au/F_{16}CuPc Interface. *J. Appl. Phys*. **2001**, *90*, 4549-4554

[15] Floreano, L.; Naletto, G.; Cvetko, D.; Gotter, R.; Malvezzi, M.; Marassi, M.; Morgante, A.; Santaniello, A.; Verdini, A.; Tommasini, F.; *et al*. Performance of the Grating-Crystal Monochromator of the ALOISA Beamline at the Elettra Synchrotron. *Rev. Sci. Instrum*. **1999**, *70,* 3855-3864

[16] de Oteyza, D. G.; Silanes, I.; Ruiz-Oses, M.; Barrena, E.; Doyle, B.P.; Arnau, A.; Dosch, H.; Wakayama, Y.; Ortega, J.E. Balancing Intermolecular and Molecule–Substrate Interactions in Supramolecular Assemblies. *Adv. Funct. Mat*. **2009**, *19*, 259-264.

[17] de Rege, P. J. F.; Williams, S. A.; Therien, M. J. Direct Evaluation of Electronic Coupling Mediated by Hydrogen Bonds: Implications for Biological Electron Transfer, *Science* **1995**, *269*, 1409-1413